Current Biology, Volume *28*

Supplemental Information

Absence of the Spindle Assembly Checkpoint Restores Mitotic Fidelity upon Loss of Sister Chromatid Cohesion

Rui D. Silva, Mihailo Mirkovic, Leonardo G. Guilgur, Om S. Rathore, Rui Gonçalo Martinho, and Raquel A. Oliveira

A

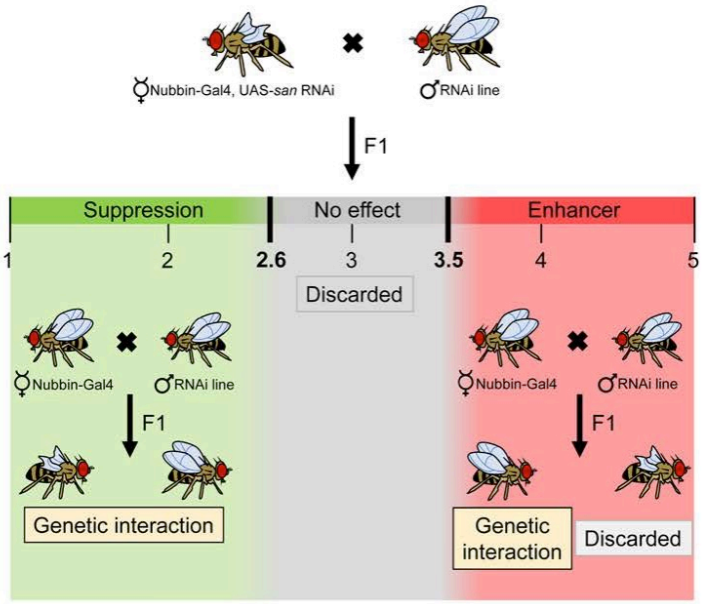

B

Type of interaction	CG	Gene	TRiP number	Average wing phenotypic class (*n*)	
				Crossed with Nubbin-Gal4	*Crossed with Nubbin-Gal4 UAS-San RNAi*
Suppressors	CG31009	*Cad99C*	HMS01451	1.00 (240)	2.35 (353)
	CG3399	*capu*	HMS00712	1.00 (161)	2.40 (170)
	CG4625	*Dhap-at*	HMC03654	1.00 (189)	2.49 (211)
	CG3265	*Eb1*	HMS01568	1.00 (175)	2.44 (232)
	CG31613	*His3*	GL00255	2.56 (223)	2.48 (123)
	CG10133	*JMJD7*	HMS00578	1.00 (232)	2.50 (263)
	CG4029	*jumu*	HMS02839	1.00 (186)	2.44 (252)
	CG17498	*mad2*	GLC01381	1.08 (202)	2.04 (224)
	CG7643	*Mps1*	GL00184	1.00 (238)	2.22 (364)
	CG34139	*Nlg4*	HMS01710	1.04 (198)	2.50 (221)
	CG40411	*Parp*	GL00229	1.00 (92)	2.21 (109)
	CG11739	*Sfxn1-3*	HMS01674	1.00 (186)	2.58 (361)
	CG5589	-	HMS00325	2.04 (257)	2.70 (155)
	CG3842	-	HMC02378	1.03 (223)	2.05 (250)
	CG31730	-	HMS02540	1.68 (133)	2.24 (269)
	CG11388	-	HMS02633	1.00 (201)	2.37 (336)
	CG4766	-	HMC02404	1.91 (204)	2.36 (287)
	CG8746	-	HMS02863	1.95 (125)	2.34 (201)
	CG12592	-	GL00498	1.00 (183)	2.48 (382)
	CG7838	*BubR1* *	GL00236	1.01 (188)	2.29 (226)
	CG7838	*BubR1* *	GLV21065	1.00 (163)	2.01 (242)
	CG2072	*mad1* *	GLV21088	1.00 (168)	2.04 (261)
	CG2072	*mad1* *	HMC03671	1.87 (120)	2.29 (232)
Enhancers	CG6875	*asp*	GL00108	1.00 (262)	4.49 (216)
	CG42312	*cno*	HMS00239	1.04 (245)	3.81 (236)
	CG32251	*Claspin*	HMS00772	1.00 (168)	4.27 (182)
	CG8598	*eco*	GL00528	1.00 (191)	4.29 (181)
	GC4203	*Mau2*	HMS02374	1.00 (122)	3.72 (182)
	CG15438	*MFS18*	HMS00961	1.00 (102)	3.98 (164)
	CG2163	*Pabp2*	HMS00553	1.00 (153)	3.91 (206)
	CG3157	*γTub23C*	GL01171	1.05 (229)	3.54 (254)
	CG9773	-	HMS01044	1.11 (192)	4.12 (124)
	CG32243	-	GL00501	1.00 (244)	3.79 (254)
	CG4274	*fzy* *	HMS00964	1.00 (113)	3.69 (258)
	CG2508	*cdc23* *	HMJ23608	1.00 (133)	3.93 (113)

Figure S1. A *Drosophila* enhancer/suppressor screen identifies several genes whose depletion modifies wing development after cohesion defects. Related to Figure 1 and Table S1

A. Crossing scheme used for the *Drosophila* wing modifier screen. Nubbin-Gal4, UAS-*san* RNAi females were crossed with males carrying different RNAi lines. The progeny of this cross was classified into five different classes according to the adult wing phenotypes described in Figure 1D and [S1]. The average adult wing class for each condition was always calculated using more than 50 adult flies (n≥50). If the average wing class for a given genetic interaction was equal or below 2.6 the RNAi line tested was classified as suppressor, if the average class was equal or above 3.5 the RNAi line was classified as an enhancer. To exclude RNAi lines whose expression by itself lead to wing morphological defects, in otherwise wild-type imaginal discs, we crossed all RNAi lines identified in the first cross with nubbin-Gal4. RNAi lines that had previously been identified as enhancers but produced significant phenotypes alone were discarded. All tested RNAis and scored adult wing phenotypes are shown in the Souce Data file. **B.** List of genetic modifiers of *san* RNAi wing phenotype. The gene abbreviations used in this figure are from Flybase version FB2017_06. The RNAi GL00255 also theoretically depletes the histone H3 isoforms CG33833, CG33806, CG33839, CG33827, CG33854, CG33824, CG33818, CG33830, CG33863, CG33815, CG33866, CG33836, CG33803, CG33851, CG33809, CG33821, CG33845, CG33857, CG33848, CG33860, CG33842 and CG33812 and the RNAi HMJ23608 also theoretically depletes CG31687, a poorly expressed chimeric gene between *cdc23* and CG31688. The gene CG5589 was classified as suppressor due to the strong adult wing phenotype of the correspondent RNAi when expressed in the wing imaginal discs with nubbin-Gal4 and the genetic interaction with *eco* and *Mau2* has been previously described in [S1]. The genetic interactions marked with an asterisk (*) were identified by a candidate gene approach. Results are mean of three independent crosses.

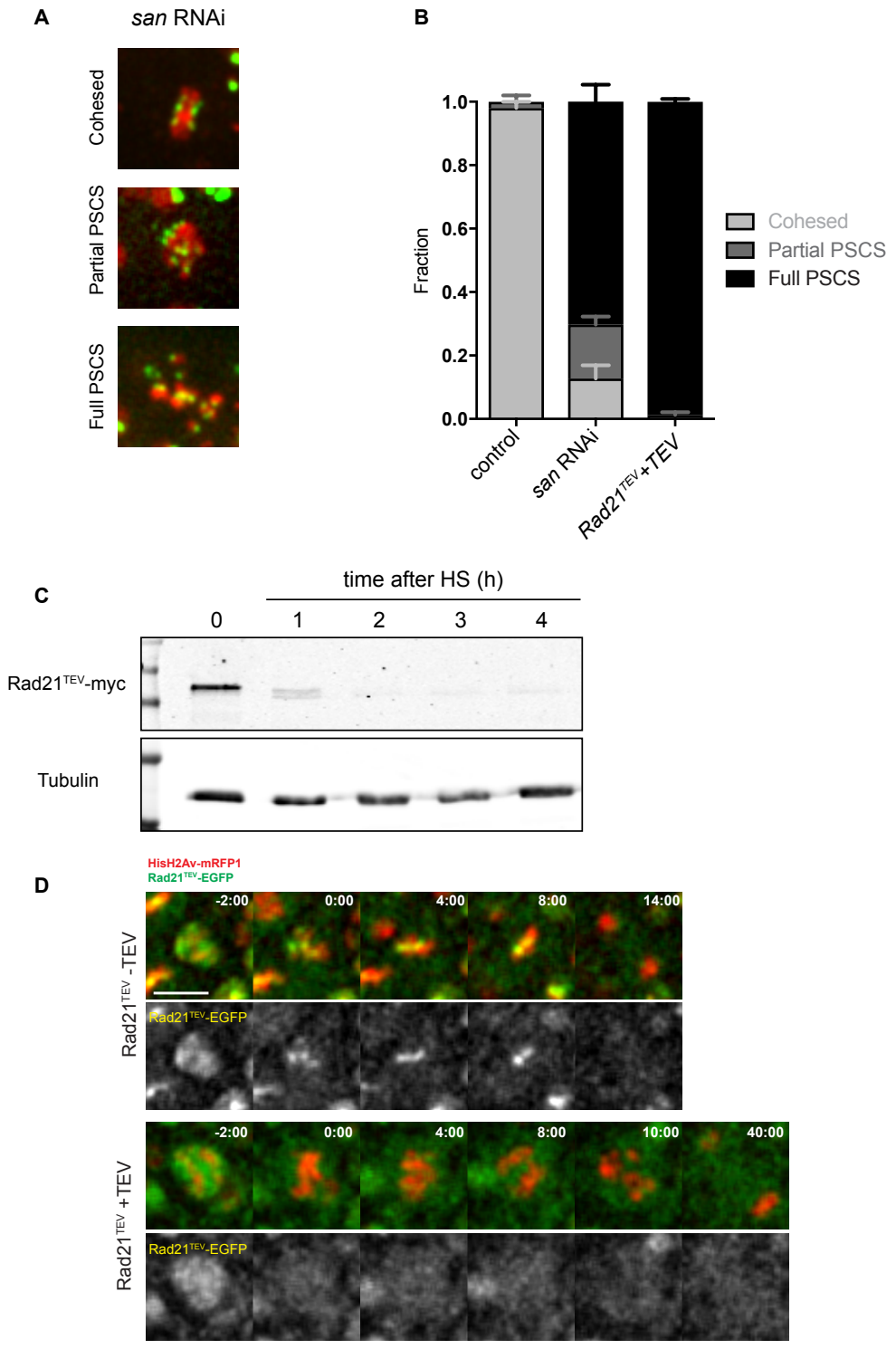

Figure S2. Premature sister chromatid separation upon San RNAi and TEV-mediated Rad21. Related to Figure 2 A. Representative images of mitotic cells from *san* RNAi undergoing mitosis with variable degrees of sister chromatid separation. Scale bar is 5 μm and applies to all images. **B.** Quantification of premature sister chromatid separation in the different experimental conditions; graph represents mean ± SEM of errors of individual discs (n≥5 independent discs corresponding to over 100 cells analysed per experimental condition). **C.** Western blot analysis of Rad21^{TEV}-EGFP levels before and after heat shock-induced TEV protease expression, probed with an anti-Rad21 antibody. Each lane corresponds to 10 dissected wing discs; anti-a-tubulin was used as loading control. **D.** Live-cell imaging analysis of strains surviving on Rad21^{TEV}-EGFP (green) without and with heat-shock induced TEV protease expression. Cells also express HisH2AvD-mRFP1. Times are relative to NEBD and scale bar is 5 μm and applies to all images.

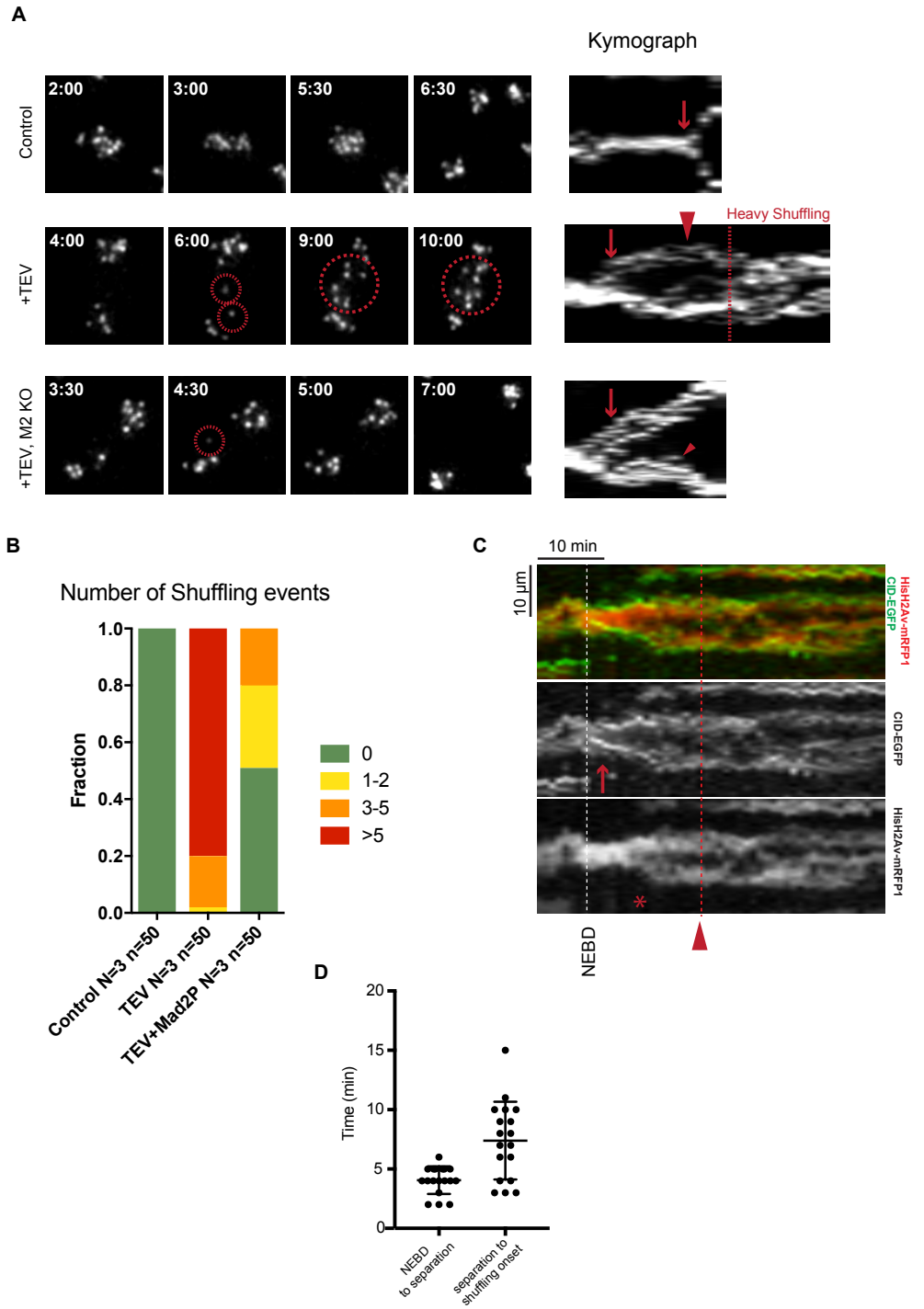

Figure S3. Analysis of frequency and onset of chromosome shuffling events. Related to Figure 3. A. Representative images centromere behaviour (Cid-EGFP) from embryos surviving solely on Rad21^{TEV} that were either non-injected (top), injected with TEV protease (+TEV) or injected with TEV protease in mad2^{P} embryos. Shuffling events were classified as each time centromeres were seen invading and/or crossing the middle of the segregation plane (dashed circles). Right panels depict the corresponding kymographs. **B.** Frequency of chromosome shuffling events quantified as in exemplified in A. **C.** Kymograph of HisH2AvD-mRFP1 and CID-EGFP of nuclei entering mitosis upon TEV-mediated cohesin cleavage in a SAC-competent wing disc cell. Scale bars are 10 min and 10 µm. Note that centromere separation (arrow) precedes chromosome individualization (*). Onset of chromosome shuffling is also indicated (arrowhead) **D.** Quantification of time between NEBD and centromere separation and centromere separation and the onset of chromosome shuffling in wing disc cells, upon TEV-mediated cohesin cleavage, relative to NEBD. Each dot represents a single cell derived from 4 independent wing discs.

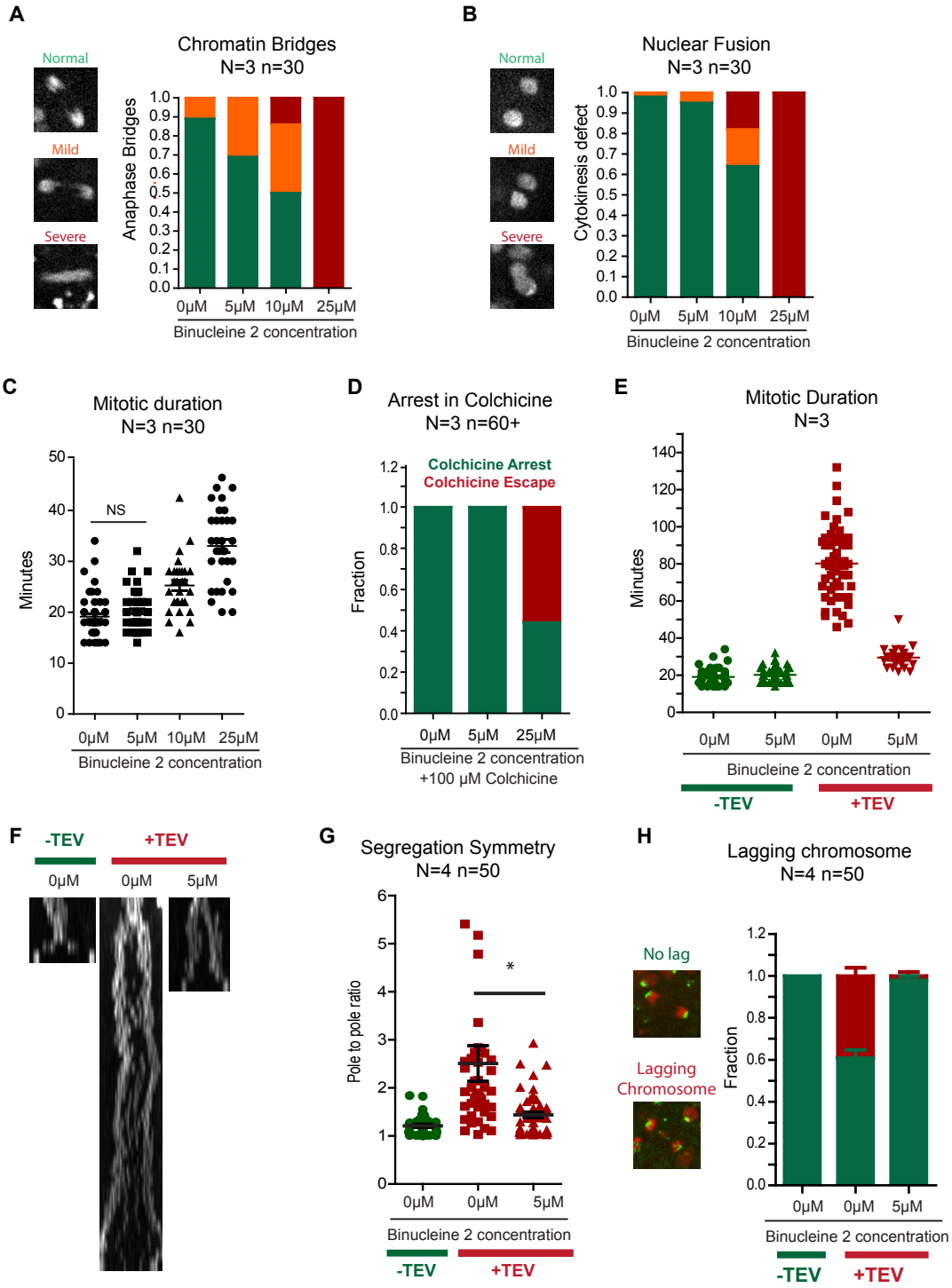

Figure S4. Aurora B inhibition prevents chromosome shuffling and improves mitotic fidelity upon cohesin cleavage. Related to Figure 3. A-D. Titration of Binucleine 2 concentration (0-25μm) to examine the inhibitor dose effect on chromosome condensation, nuclear separation, mitotic duration and SAC competency in control cells. Still images from live imaging of the wing disc pouch. Graphs depict frequencies or time (in minutes), N represents the number of independent wing discs and n the number of analyzed cells. **E**. Mitotic duration of control, TEV cleavage and TEV+B2 incubated wing disc cells. N represents the number of independent wing discs and each dot corresponds to a single cell. **F.** A kymograph representing centromere positioning (Cid-EGFP) from Control, TEV cleavage, and TEV cleavage with 5μM Binucleine incubation. **G**. Segregation symmetry of control, TEV cleavage and TEV+ 5μM B2 incubated wing disc cells **H**. Lagging chromosome at anaphase frequency for control, TEV cleavage and TEV+B2 incubated wing disc cells.

Table S1 - Main function of the genes identified in the screen. Related to Figure 1

CG	Gene	Human/Yeast orthologue	Description	Type of interaction	References (PMID)
CG6875	*asp*	ASPM/ -	Mitotic microtubule organization	Enhancer	10073938
CG31009	*Cad99C*	PCDH15/ -	Cell adhesion	Suppressor	11162110
CG42312	*cno*	AFDN/ -	Cell adhesion	Enhancer	22024168
CG3399	*capu*	FMN2/ -	Nucleation of actin microfilaments	Suppressor	17925229
CG32251	*Claspin*	CLSPN/ -	DNA replication checkpoint	Enhancer	22796626
CG4625	*Dhap-at*	GNPAT/ -	Peroxisomal ether lipid synthesis	Suppressor	22758915
CG3265	*Eb1*	MAPRE1/ BIM1	Spindle assembly, dynamics, and positioning	Suppressor	12213835
CG8598	*eco* [1]	ESCO1/ECO1	Cohesion establishment	Enhancer	14653991
CG31613	*His3*	HIST1H3B/ -	Chromatin component	Suppressor	
CG10133	*JMJD7*	JMJD7/ -	Putative histone demethylase	Suppressor	
CG4029	*jumu*	FOXN4/ -	Transcription factor	Suppressor	10940625
CG17498	*mad2*	MAD2L1/ MAD2	Mitotic spindle checkpoint	Suppressor	15075237
CG4203	*Mau2* [1]	MAU2/ -	Cohesion loading	Enhancer	10882066
CG15438	*MFS18*	SLC17A9/ -	Major facilitator superfamily transporter	Enhancer	22359624
CG7643	*Mps1*	TTK/ MPS1	Spindle checkpoint	Suppressor	15556864
CG5589	-	Ddx52/ ROK1	ATP-dependent RNA helicase	Suppressor	28701701
CG3842	-	-/ ENV9	Retinoid-active short-chain dehydrogenase/reductase	Suppressor	19520149
CG31730	-	-/ -	N-terminal acetyltransferase [2]	Suppressor	
CG11388	-	XXYLT1/ -	Protein glycosylation [3]	Suppressor	
CG4766	-	Mab21l2/ -	Cell fate [4]	Suppressor	
CG8746	-	-/ -		Suppressor	
CG9773	-	UNC50/ GMH1	UNC-50 protein family	Enhancer	
CG32243	-	-/ -		Enhancer	
CG12592	-	SLAIN1-2/ -		Suppressor	
CG34139	*Nlg4*	NLGN3/ -	Synaptic adhesion protein	Suppressor	10892652, 24068821
CG2163	*Pabp2*	PABPN1/ SGN1	mRNA polyadenylation	Enhancer	10481015
CG40411	*Parp*	PARP1/ -	DNA repair/transcription	Suppressor	11376691, 24055367
CG11739	*Sfxn1-3*	SFXN1/ FSF1	Mitochondrial ion transmembrane transporter	Suppressor	
CG3157	*γTub23C*	TUBG2/ TUB4	Microtubule organization	Enhancer	1904010

[1] The genetic interaction with *eco* and *Mau2* has been previously described [S1].
[2] Testis specific paralogue of *Drosophila* Naa20 (CG14222).
[3] Homologue to the human xyloside xylosyltransferase 1 that transfers the second xylose to O-glucosylated epidermal growth factor repeats of notch
[4] Paralogue of *Drosophila* mab-21 (CG4746).

Supplemental References:

S1. Ribeiro, A.L., Silva, R.D., Foyn, H., Tiago, M.N., Rathore, O.S., Arnesen, T., and Martinho, R.G. (2016). Naa50/San-dependent N-terminal acetylation of Scc1 is potentially important for sister chromatid cohesion. Sci Rep *6*, 39118.